Engineering and Technology Journal 40 (11) (2022) 1589- 1604

Engineering and Technology Journal
Journal homepage: https://etj.uotechnology.edu.iq

Dynamic Response of Deepwater Pile Foundation Bridge Piers under Current-wave and Earthquake Excitation

Riyadh Alsultani [a], Ibtisam R. Karim[a], Saleh I. Khassaf [b]

[a]Civil Engineering Dept., University of Technology-Iraq, Alsina'a street, 10066 Baghdad, Iraq.
[b]Civil Engineering Dept., University of Basrah, Basrah 61001, Iraq.
*Corresponding author Email: bce.19.52@grad.uotechnology.edu.iq

HIGHLIGHTS

- The major methods for investigating the interaction between a wave current and an elevated pile cap foundation are discussed.
- The changing rule of hydrodynamic pressure with water depths, current speed, wave properties, earthquake amplitudes, and frequencies are presented.
- A series of combined current-wave-earthquake tests are shown.

ARTICLE INFO

Handling editor: Mahmoud S. Al-Khafaji

Keywords:
Nonlinear dynamic analysis; current-wave-earthquake; coupled Matlab-Abaqus; bridge pier; hydrodynamic pressure.

ABSTRACT

Pile foundation bridges are structures extending in the middle of the sea, so they are subject to currents, waves, and earthquake forces**.** This article presents a hybrid simulation that was used with input excitations of different current velocities, wave properties, and earthquake amplitudes to assess the non-linear dynamic behavior of pile foundation bridge piers. Based on the interface between MATLAB and ABAQUS software, the general formulations of fluid-structure interaction (FSI) under combined current-wave and earthquake loads are derived. Hydrodynamic and earthquake loading is consistently introduced by creating synthetic time histories of combined current-wave actions and spatially variable ground motion. The behavior of the dynamic model of a deepwater pile foundation bridge for the Songhua River in northeast China was adopted as an example of the study. The accuracy of the created model was verified using prior experimental and analytical computations. It is demonstrated how both linear and nonlinear dynamic behavior performs at various water depths under coupled current-wave-earthquake loading conditions. Revealing interesting aspects, particularly in terms of relative displacement, acceleration, shear, and moment response are shown. The results showed that the hybrid model is an efficient of simulating accurate predictions of the hydrodynamic pressure during earthquake actions for structures in coastal areas.

1. Introduction

Large-span bridges across rivers, seas, straits, or oceans are frequently crossed using pile foundation bridges. Due to their structural efficiency, low cost, and ease of construction, pile foundations have become frequently employed in deepwater multi-long span bridges in recent years (AbdelSalam et al. [1], Wei et al. [2]). The major component of a bridge's foundation is a group of long piles that reach the ground below the water's surface and are joined by a substantial concrete top. The majority of these foundations include pile caps that are partially or completely buried in the water in addition to the piles, which adds to the consequences of the produced dynamic fluid-structure interaction (Wei et al. [2]). Such types of these bridges are situated in areas with high seismic hazard ratings, where they are not only vulnerable to earthquakes but also ordinary current-wave stresses. Excitation of an earthquake may raise the hydrodynamic pressure on the portion of the bridge that is submerged, thereby greatly raising the risk of structural failure [3-5].

Fluid-structure interaction (FSI), which does not apply to ordinary bridges, must be considered when designing deepwater bridges for coastal environments. The analytical solutions of the free vibration and natural frequencies of columns surrounded by water were developed by Usciowska and Koodziej [6]. In a full-scale experiment, Yue and Bi [7] investigated the vibration problem brought on by sea impact on the structure. Zhang [8] used a discontinuous deformation analysis approach and simulated the dynamic interaction process between sea ice and vertical structures. Liu [9] studied the dynamic response of pier structures under earthquake and sea wave stresses using the finite element approach. Huang [10] looked at the dynamic properties and the extent to which the dynamic response of the water and pier during seismic excitation affected the pier structure. Gao [11] investigated the effect of hydrodynamic added mass on deep water bridge seismic response to various types of seismic activity.

http://doi.org/10.30684/etj.2022.135776.1285
Received 26 September 2022; Accepted 22 October 2022; Available online 21 November 2022
2412-0758/University of Technology-Iraq, Baghdad, Iraq

Pei [12] investigated the seismic dynamic response of the Hardfill dam using new quality requirements and FSI theory. The above studies showed that when current waves and earthquakes were coupled, the dynamic reactions were more substantial than when earthquakes were alone, and the dynamic assessments under wave motion cannot be ignored.

For submerged columns, many simplified equations were derived by (Li and Yang [13] and Yang and Li [13]). Wei et al. [2] used PBFEs to perform modal analysis on pile foundations submerged in water, and the results of the experiments were used to validate the numerical model. The authors have also created additional mass models for an immersed column's inner and outer waters with a circular hollow cross-section (Jiang et al. [14]). The widespread use of submerged columns with complicated geometry other than circular cross-sections is facilitated by the ongoing advancement of offshore engineering (Wang et al. [15]). To study the damage characteristics of dams, Wang et al. [16] employed the Lagrange formulation of fluid in the reservoir-dam-foundation numerical model. The boundary element method (BEM) has also been used to shed light on the FSI problems in the engineering sectors (Xu et al.[17], Liu [18]). The mentioned researcher approved that the seismic response of the submerged bridge members is amplified because of the hydrodynamic pressure effect. Currently, FSI research into the effects of earthquakes focuses mostly on the influence of still water on the structure and the reaction to earthquakes in deep water.

Numerical modeling plays an important role in understanding the complex FSI phenomenon and designing marine structures. A typical feature of numerical modeling in FSI problems is simultaneously considering strong earthquake excitation and current-wave interaction and small-scale physics in the near field of the structures, such as nonlinear fluid-elastic structure interactions (Jiang et al. [14]). In the last decade, there has been an increasing interest within the numerical modeling community to improve the modeling aspects by coupling different methods to take advantage of different approximations for practical problems or to model large domains/durations. Such hybrid approaches would reduce the computational time within high-performance computing by maintaining high fidelity. It can be either one-way (weak) or two-way (strong), depending on the problem. Recent international numerical comparative studies and literature have confirmed the promising superiority of hybrid modeling over conventional single-model approaches (Gou et al. [19]). Although the dynamic response of deepwater bridges can now be calculated using a hybrid FSI numerical approach, most of these techniques have not yet been fully integrated into standard engineering practice, particularly for the coexistence field, such as the combined current-wave-earthquake flow field. They call for specialized software, advanced programming, and high-level expertise.

Under intense earthquakes, a deepwater bridge pier may yield and enter a nonlinear condition (Jiang et al. [20], Pang et al. [21]) performed fragility assessments on a multi-span coastal bridge and discovered increased damage, which was likely caused by deeper water. Jiang et al. [14] used the added-mass model to conduct fragility assessments for a deepwater continuous rigid-frame bridge and discovered that the hydrodynamics might increase the risk of damage and nonlinear deformation for the analyzed piers. The seismic evaluations of deepwater pile foundation bridges must consider both geometrical and material non-linearity. Few studies have used numerical modeling to solve this issue.

Because of its ease and simplicity, the added-mass model has been widely utilized in design practice and research since it was originally employed by Westergaard [22] to evaluate the hydrodynamic effect on the dam. The works of Li and Yang [23], Jiang et al. [14], and Wang et al. [15] present several added-mass models for deepwater cylindrical and elliptical piers. The added-mass model for the intricate hollow pier with a rectangular cross-section, frequently utilized in practice, has, however, received less attention (Gou et al. [19]). The added-mass method's applicability in nonlinear analyses has to be determined because the current research about its verification is restricted to the linear seismic responses of deepwater piers.

This paper investigates non-linear bridge pier dynamic response in the nested current-wave-earthquake domains-induced hydrodynamic pressure by the hybrid numerical method based on the integration between MATLAB and ABAQUS software. First, the created model for the efficiency of the pile foundations was verified using prior experimental and analytical computations. Then, under various water depths, the bridge pier's relative displacement, acceleration, shear, and moment were computed and compared. In addition, the loading conditions were used to show the bridge pier's linear and nonlinear dynamic behavior.

Finally, a typical multi-span pile foundation bridge was selected as a case study to find the 3D hydrodynamic forces combined with earthquake actions.

2. Materials and Methods

2.1 Case Study Definition

The pile foundation of a continuous bridge crossing the Songhua River in northeast China was taken as a case study structure in Figure 1 (Wei et al. [2]). The bridge foundation consists of nine concrete circular piles with a length of 12m above the scour line and a diameter of 1.8m. It also includes a concrete square pile-cap with dimensions of $12 \times 12 \times 3$ m, a rectangular concrete pier with dimensions of 4.8×3 m, a concrete hammer-shaped pier-cap with a height of 3m, a concrete superstructure, and the other elements of the superstructure. The superstructure, pier, and pile-cap were constructed using Chinese Grade C35 concrete, with Young's modulus of 31.5GPa. The piles were constructed using C25 concrete, with Young's modulus of 28GPa (Ministry of Communications of China 2007)[24].

2.2 Modeling Technique

This work aims to create a hybrid numerical model that can precisely predict how the pile foundation bridge will behave when subjected to combined current-wave and earthquake accelerations.

It takes an FSI model to do this. The governing equations for the structural solver and fluid solver are precisely described in this section. The dynamic response of the bridge is examined using a structural solver in the current study, while the hydrodynamic forces are examined using a fluid solver. For FSI simulation, MATLAB and ABAQUS were utilized as commercial programmers.

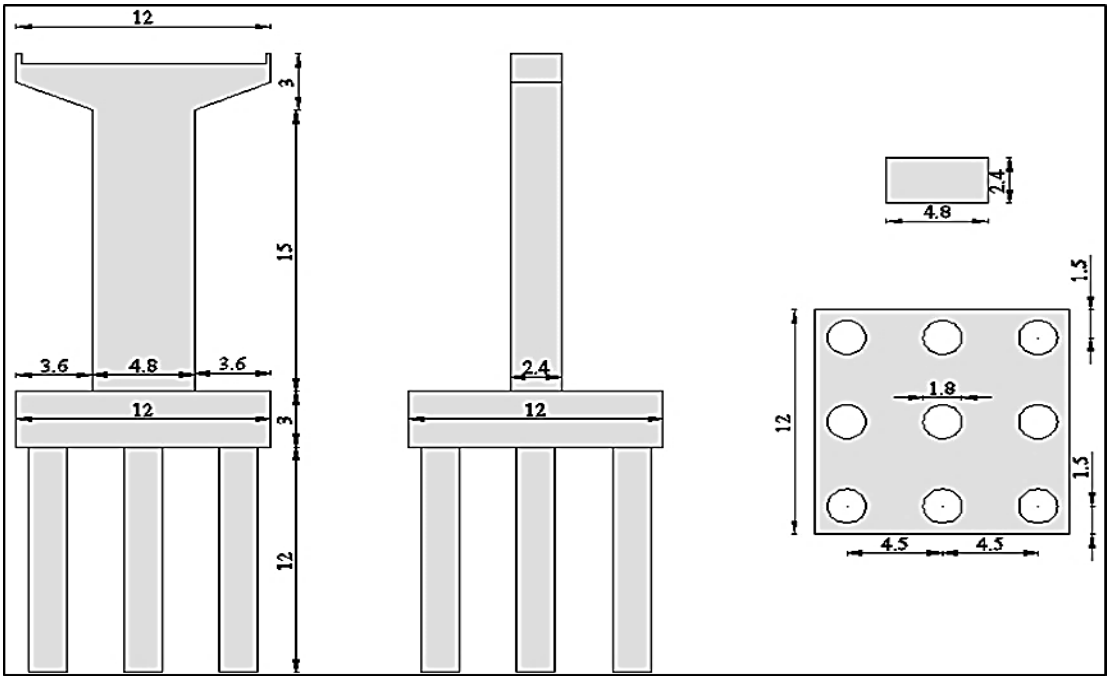

Figure 1: The geometry of the selected case study Wei et al. [2] (All dimensions are in meters)

The computational time and force calculation are one of the main drawbacks to a comprehensive numerical analysis of the current wave effect in particular and dynamic seismic loads in general. As a result, in addition to exact model combinations, time and computing needs are critical factors. The ability to perform such challenging simulations has increased exponentially due to advances in technology and software.

The suggested model was created in the general-purpose finite element software ABAQUS utilizing a coupled Eulerian-Lagrangian (CEL) analysis. To simulate interactions between highly flexible materials and relatively rigid bodies, classical Lagrangian formulations can be combined with the Eulerian capabilities offered by ABAQUS (Xu et al.[17]). The two-way FSI coupling drastically cuts down on time needed to analyze FSI issues. The structure solver is represented by the transient structural module and the fluid solver by the Eulerian module. However, FSI issues are frequently complicated. An algebraic equation system is produced by discretizing the mathematical model in time and space and integrating time for the fluid flow and structural domains. In this case, loads are switched from the structure to the fluid at the interface and vice versa. As a result, the mesh must be modified at each stage of the solution because the boundary conditions change. Although the general momentum equation applies to fluids, transient analysis cannot use it since the solution domain constantly shifts. As a result, the mesh has to be adjusted to the new flow boundary. A relative velocity that compares the real fluid velocity to the mesh velocity takes the place of the real fluid velocity for a constant mesh. So that the mesh updates each time, the momentum equation is modified Gruber [25]. The dynamic mesh model is used by ABAQUS-Eulerian to simulate flows where the domain's shape changes over time due to motion at its borders. The dynamic mesh simulates flows when the solid domain's boundaries move, and the domain changes over time.

When a bridge is in the ocean and suffers from currents-waves and earthquakes, and the hydrodynamic force acts as an external force on the bridge, the governing equation of transient structural dynamics can be refined as:

$$[M]\{\ddot{x}\ (t)\} + [C]\{\dot{x}\ (t)\} + [K]\{x\ (t)\} + [M]\{\ddot{x}_g\ (t)\} = \{F_H(t)\} \quad (1)$$

where $[M]$, $[C]$, and $[K]$ represent the structural mass matrix, damping matrix, and stiffness matrix, respectively. $\{x\ (t)\}$, $\{\dot{x}\ (t)\}$ and $\{\ddot{x}\ (t)\}$ represent the relative structural displacement, velocity, and acceleration vectors, respectively. $\ddot{x}_g\ (t)$ is the acceleration vector of seismic ground motion. $\{F_H(t)\}$ is the fluid force vectors exerted on the bridge structure, including wave-current force and earthquake-induced hydrodynamic forces.

MATLAB was used to model the bridge using reinforced bars. Bridge concrete has a density of 2400 kg/m^3 and a toxicity ratio of 0.18 Liu [18]. SOLID186 solid elements, a higher-order 3D 20-node solid element, are used to model this concrete. This element exhibits the displacement behavior of second-class, which is characterized by 20 nodes with three degrees of freedom each. The element enables creep, big deflection, strain capacities, hyper-elasticity, plasticity, and stress stiffening.

The finite element method (FEM) can discretize the structural governing equation. Meanwhile, the general governing equations of fluid dynamics (e.g., Eulerian-Lagrangian equations) are discretized using the finite volume method (FVM). In the numerical model, the interface implements the mutual real-time feedback of the calculation results between the fluid field and structure. This coupling process can be described in detail as the structure in water will generate deformations because of fluid pressure. Meanwhile, the motional structure with rigid body displacement and deformation will affect the fluid field, and the distribution and magnitude of fluid pressure will be changed accordingly.

The final results are obtained by multiple iterations with an advanced numerical method conducted by MATLAB combined with CEL in the ABAQUS Workbench platform. Where the simulation is performed between Transient Structural (MATLAB) and Fluid Flow (ABAQUS), both modules are developed independently and connected through the system coupling module to make a two-way fluid-structure coupling computational framework.

While the Eulerian and Lagrangian components are coupled via penalty techniques, the general contact approach automatically computes and tracks the interface between the Lagrangian structure and the Eulerian materials Abaqus [26]. Solid components are used to simulate the piles, pile top, pier, and bridge deck. To simulate the structural parts, specifically, 3D elements with restricted integration and hourglass control are employed. Figure 2 introduces the two-way FSI analysis's flow between ABAQUS and MATLAB.

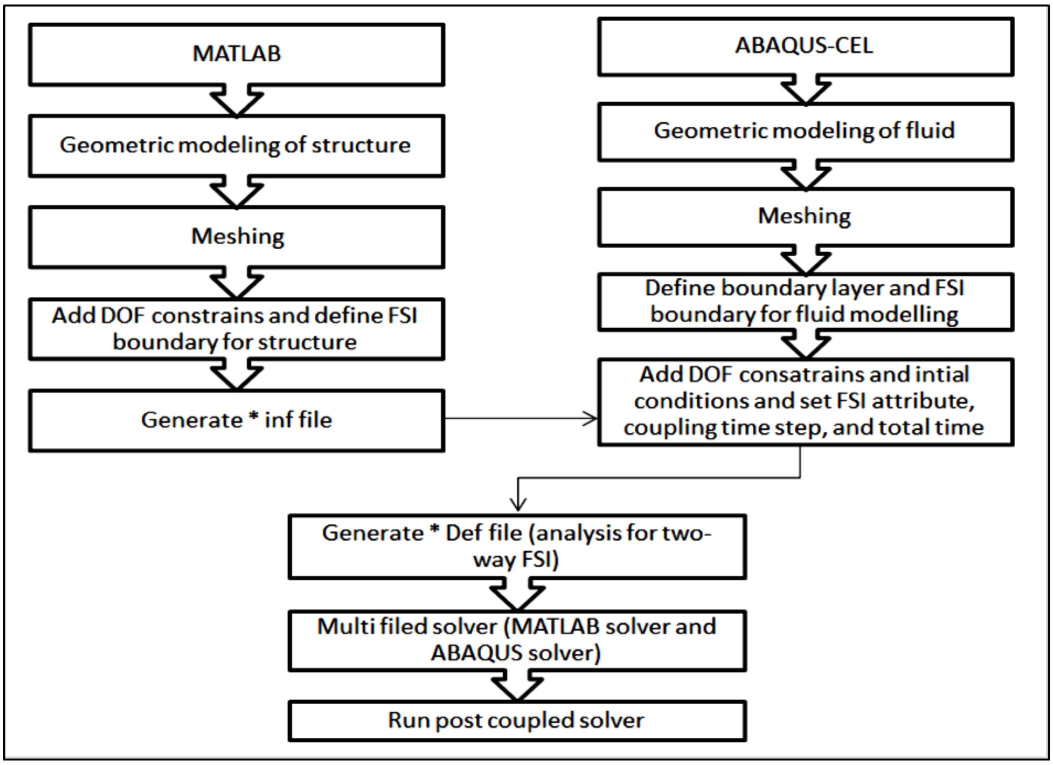

Figure 2: The scheme of the MATLAB-ABAQUS two-way FSI analysis

2.2.1 Wave and current generation

The volume of fluid (VOF) method is used to track the free-surface profile by introducing a fluid volume fraction a_q. a_q denotes the ratio of the volume occupied by the q-phase fluid to the total volume, whose value is between 0 and 1 (including 0 and 1). When $a_q = 1$, the q-phase substance is full, when $a_q = 0$, the q-phase substance is empty, and when $0 < a_q < 1$, it means that the multiphase flow interface. For example, for the two-phase flow patterns of air and water in this paper, there are the following relationships:

$$\frac{\partial a_q}{\partial t} + \frac{\partial(u a_q)}{\partial x} + \frac{\partial(v a_q)}{\partial y} + \frac{\partial(w a_q)}{\partial z} = 0 \qquad q = 1,2 \tag{2}$$

$$\sum_{q=1}^{2} a_q = 1 \tag{3}$$

In which u, v, and w are the fluid velocity components in x, y, and z directions, respectively. Wave generation adopts the boundary-generating wave method by defining analytical expressions of the velocity and the wave surface, which vary with time at the inlet boundary. This method has strong operability and a wide application range and is particularly convenient for simultaneous wave and current generation. For this case, it only needs to superimpose current velocity components based on wave velocity components at the inlet boundary. Fluids are forced to make periodic alternating movements in a specified form at the inlet and outlet boundary defined by opening velocity, which can eliminate wave reflections from the outlet boundary. And the relative static pressure is set as zero at the top boundary defined by opening pressure. Both side surfaces of the flume are defined as symmetric boundary conditions, while the bottom of the flume is defined as a no-slip wall. The pile-pier-water coupling surface transfers real-time data between the bridge pile and the flow field. The initial conditions of the transient calculation can be set up by compiling CEL codes according to the preset wave velocity, wave surface profile, and corresponding hydrostatic pressure to save the iterative calculation time for forming a stable wave field. Mesh refinement is applied to the whole applied water shape with 0.005m Hexa/Quad., and contains 6556–7686 elements in their mesh statistics, and there are between 318 and 412 boundary elements.

In the calculation model for a water-air two-phase flow of compressible viscous fluids, the water density is $\rho_f = 1000$ kg/m^3, the dynamic viscosity of water is $\mu_f = 0.8899\times10^3$ Pa s, the air density is $\rho_a = 1.185$ kg/m^3, the dynamic viscosity of air is μ_f = 1.831×10^5 Pa s, the reference pressure is 1atm = 101325Pa (i.e., a standard atmospheric pressure), and the surface tension coefficient is 0.0725N/m ,Liu, 2019[18].

2.2.2 Earthquake generation

The bottom of model piles fixed with a seabed moves synchronously with the seabed, and earthquake excitation is conducted by the user-defined function in the ABAQUS-CEL module. If a seismic excitation input to the seabed tied up with the bottom of the pile is the displacement time history of the seismic wave, the absolute structural displacement (including rigid and elastic displacement) will be obtained, and then the hydrodynamic force exerted on the structure consists of two parts, namely the one generated by rigid motion and the other one generated by elastic vibration. On the other hand, if a seismic acceleration time history is applied to the entire structure and the bottom of piles remains stationary, the hydrodynamic force caused only by the structural elastic vibration can be obtained. Within CEL, the standard two-equation k-epsilon model is chosen as the turbulence calculation model, the scalable wall function is used to model near the wall region, the solver's discrete format is set to high resolution, and the second-order backward Euler scheme is used for time integration.

To assess the model structure's response to earthquake excitation, the acceleration time history of the Halabjah earthquake (November 12, 2017) in Baghdad (Al-Taie and Albusoda) [27] was selected as the input earthquake excitation. The acceleration time histories for both north-south and east-west horizontal components of this earthquake excitation are shown in Figure 3. The elastic vibration-induced hydrodynamic force accounts for a large proportion of the total hydrodynamic force, noting that the aforementioned two peaks do not occur simultaneously. In other words, the maximum value of the elastic vibration-induced hydrodynamic force and the maximum value of the rigid motion-induced hydrodynamic force does not occur simultaneously. Therefore the maximum value of total hydrodynamic force can't be simply added by the two.

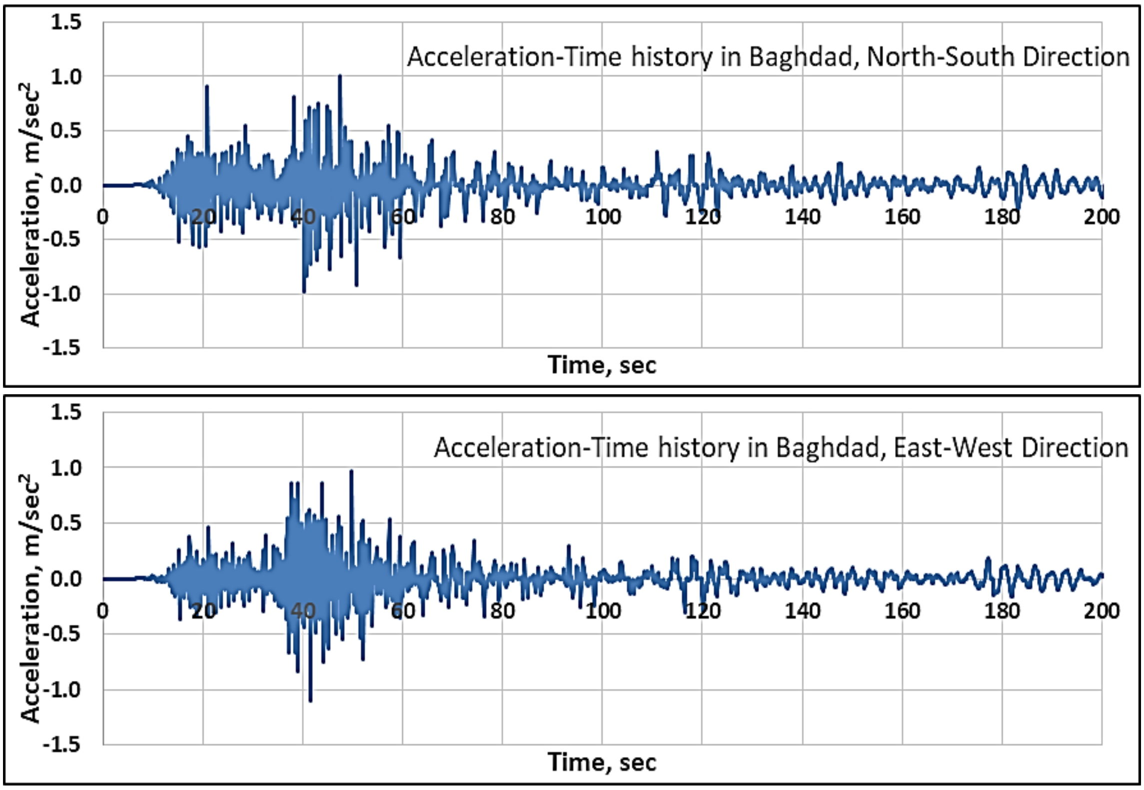

Figure 3: Time history components of the Halabjah Earthquake

2.2.3 Non-linearity

According to MCPRC [28], the example model is composed of concrete and HRB 400 rebar, as presented in Figure 4 (a and b). The concrete has an elastic modulus of 32.5 GPa, a 28-day compressive strength of 34 MPa, a Poisson's ratio of 0.2, and a mass density of 2,500 kg/m^3 accordingly Liu [18]. The rebar has 210 GPa elastic modulus, 400MPa yield strength, 0.15 failure strain, and 7,850 kg/m^3 mass density, respectively Liu [18]. The influence of the concrete's non-linearity was incorporated into the model of the example pier using the concrete material suggested by Bathe et al. [29], which has been validated and used in several prior investigations (Khatri and Anderson [30], Mao and Taylor [31]). The nonlinear characteristics of the RC pier were estimated using the restricted concrete model of Mander et al.[32] to account for the contribution of the reinforcing bars to the ductility and nonlinear behavior of the reinforced core concrete. According to the calculations of the confined concrete model, the elastic modulus E_c = 32.5 GPa, the maximum uniaxial compressive strength σ_c = 43.9MPa, the maximum uniaxial compressive strain $e_c = 0.0049$, the ultimate uniaxial compressive strength $\sigma_u = 35.8$ MPa, and the ultimate uniaxial compressive strain $e_c = 0.016$. The behavior of the concrete model in the tension zone was considered linear, and the cracks were suppressed for the simulation to converge. Figure 5 shows the RC material's completely nonlinear stress-strain relationship. The elastic modulus and mass density of the concrete were adjusted to constant values of 32.5 GPa and 2,500 kg/m^3 for the linear studies that took into account the linear behavior of the RC material. By characterizing the kinematics of the solid element as big displacement, the influence of geometric non-linearity was also integrated into the nonlinear analysis. The seismic responses of the example pier were then determined using the constructed numerical models.

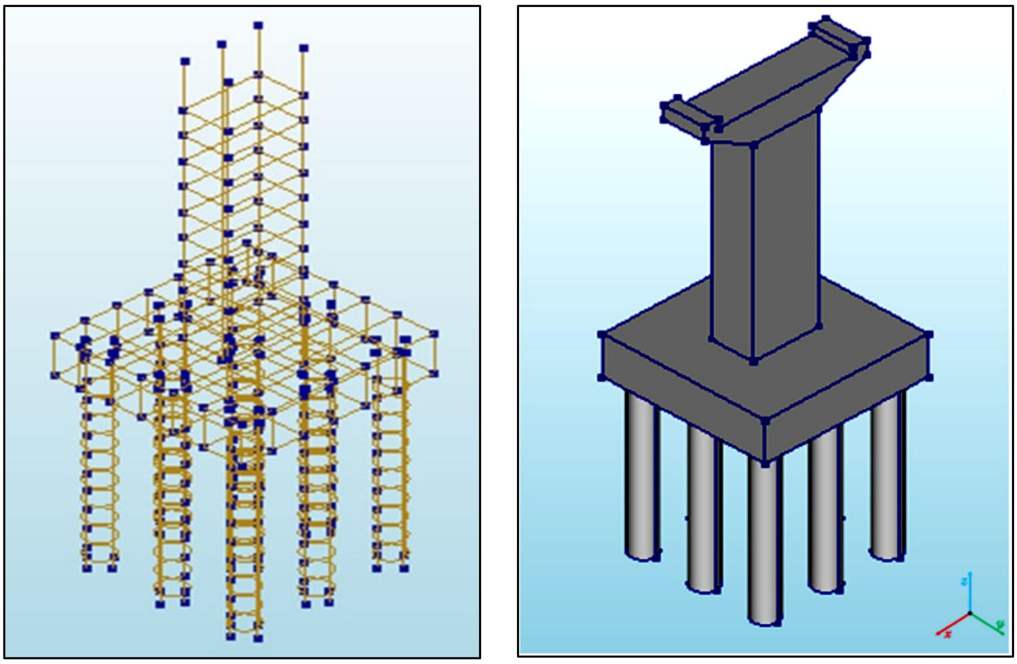

(a) Reinforcement details (b) Concrete members

Figure 4: Finite element of the example model

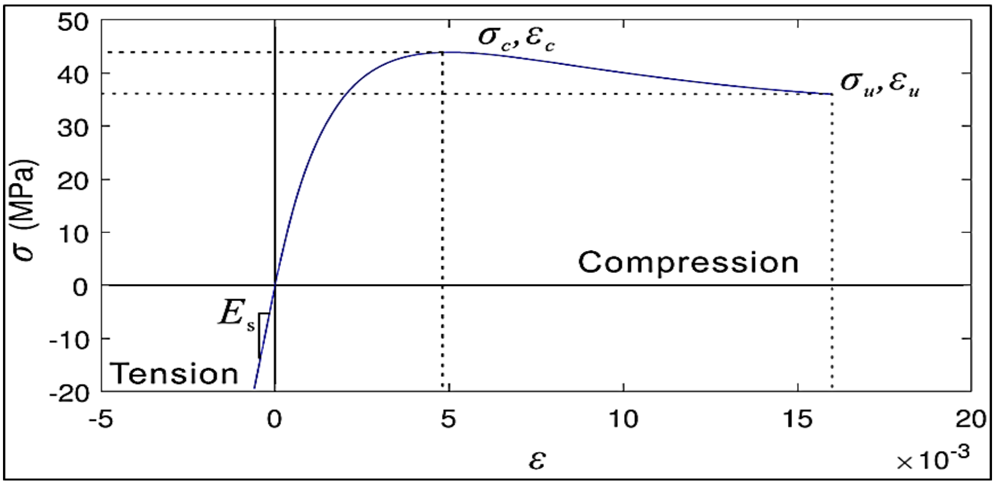

Figure 5: The nonlinear restricted concrete material uses a single stress-strain relationship

To study the forces and soil conditions that impacted the numerical model, it has been assumed that the pile group is in a state of complete stability, and this procedure was done by choosing Clamped Feet. The bridges usually carry a range of forces over their superstructure surface resulting from traffic loads and live loads as Added Mass. Earthquake actions were represented as forces affecting the bottom of the model and in both directions (X, Y, or combined), making it possible to represent the acceleration of an earthquake with the exact values. Current and wave forces were selected from a drop-down list in the interface of the Software, where they were represented programmatically by Morison's equation and along the model's height. Its values depend on the input current speed and the wave's length, width, and period.

Figure 6 shows the assumed boundary conditions for the selected pile foundation bridge pier model.

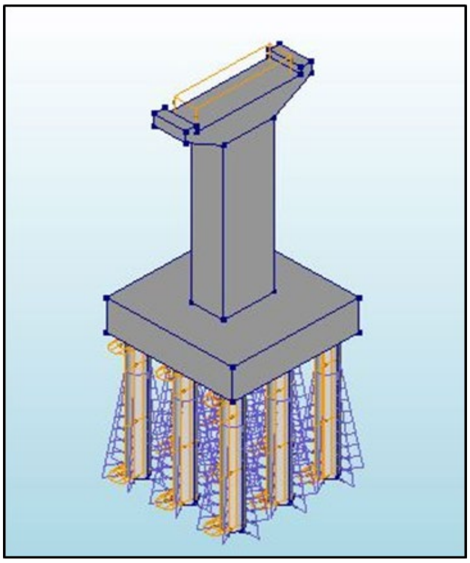

Figure 6: Boundary conditions of applied loads

2.3 Model Validation

Validation of the used methodology is undertaken based on prior experimental testing to corroborate the modeling approach. To sum up, the superposition law may be used to generate the hydrodynamic force of each harmonic motion to generate the overall hydrodynamic force under the earthquake. An earthquake motion can be broken down into a sequence of harmonic movements with various amplitudes, frequencies, and phases (Yang et al.[4]). As excitations acted on a cylinder, a harmonic motion was selected. Yang et al. [33] conducted a physical experiment result on a single cylinder vibrating in still water to validate the modeling approach's accuracy and the associated parameters. The two-way FSI analysis used to produce the hybrid FSI numerical model has the same dimensions and is subject to the same external stimulation as the physical experimental model. Figure7 illustrates the comparison of the hydrodynamic force time histories between the physical experimental model and the numerical model. It can be seen that during the first few cycles, the harmonic wave amplitudes gradually increase from 0 to 0.025 m. In contrast, the hydrodynamic force amplitudes gradually decrease from 0 to a constant value. The two curves closely coincide, demonstrating the validity of the present hybrid model's solution.

According to Eqs. (4)-(6), the added masses were calculated and allocated at nodes of the solid components below the still-water level Yang [34], Li and Yang [13], Zhang et al.[35]

$$M_{a0} = C_M \frac{\rho \pi B^2}{4}\left(1 - 5\frac{B}{H_w^2}\right)\left\{1 - exp\left[\frac{10(z_j - H_w)}{BH_w^{1/3}}\right]\right\} \quad (4)$$

$$M_{aI} = \rho B_1 L_1 \left\{1 - exp\left[\frac{5(z_j - H_w)}{B_1 H_w^{1/5}}\right]\right\} \quad (5)$$

$$C_M = 1.51(B/L)^{-0.17} \quad (6)$$

where M_{a0} and M_{aI} = added mass per unit length concerning outer and inner water, respectively; B and L = outside width and length of the rectangular hollow pier cross-section, respectively; B_1 and L_1 = inside width and length of the corresponding section, respectively; B and B_1 = dimensions of the sides perpendicular to the vibration direction; and z_j = vertical coordinate of Node j.

Current and wave are in the positive longitudinal direction, the north-south and east-west components of Halabjah selected for seismic excitation are in the direction of x and y, respectively, and the coordinate directions are shown in Figure 2. The drag coefficient C_D and inertial coefficient C_M affected by the current in the Morison equation are taken as 1.21 and 1.38, respectively, specified in the Code of Hydrology for Harbor and Waterway published by China Communications Press (2015)[36]. To get frequency-domain responses, the current hybrid FSI model is additionally subjected to harmonic ground motion acceleration with frequency ranging from 0 to 10 Hz. Figure 8 (a-d) compares the frequency responses, such as the base shear and base moment underground motion, as well as the horizontal acceleration and displacement at the pier top.

Near the first modal frequency, the FSI findings and the additional mass results agree. However, some variations between these curves may be seen towards the second mode frequency since the hydrodynamic added mass utilized in this work is a frequency-independent mass, which solely accounts for hydrodynamic force caused by stiff structural motion and neglects the influence of vibration mode.

Here, the peak structural acceleration at the pier top, displacement at the pier top, base shear at the pier bottom, and base moment at the pier bottom occur at curves obtained by the two methods that agree well. The peak values of responses and their relative errors are small and acceptable. It can be concluded that the hybrid numerical simulation method in this paper is of high accuracy and reliability as an alternative for deepwater bridge dynamic analysis.

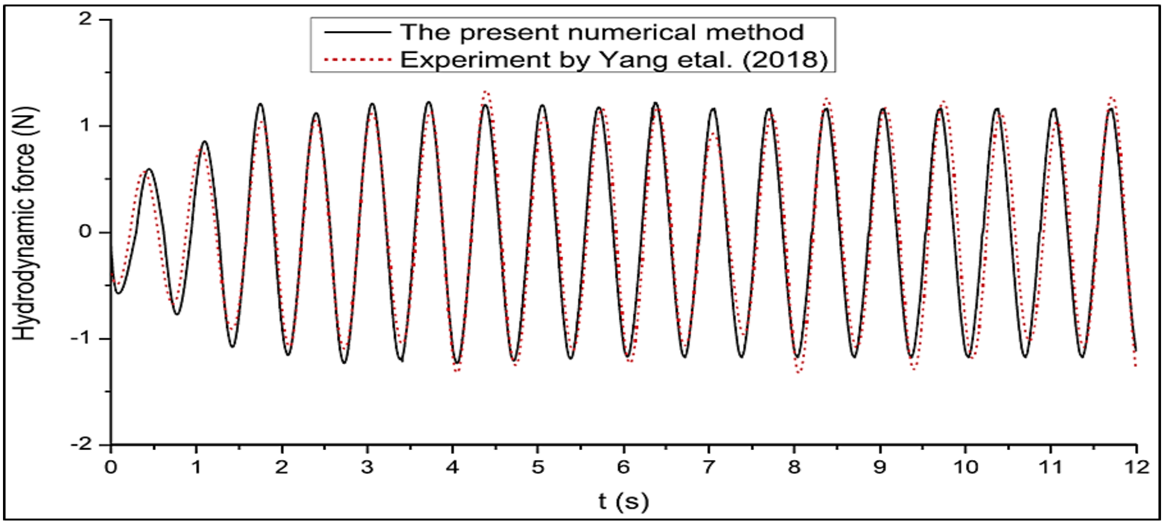

Figure 7: Confirmation of the built model by the experimental results in Yang et al. [33]

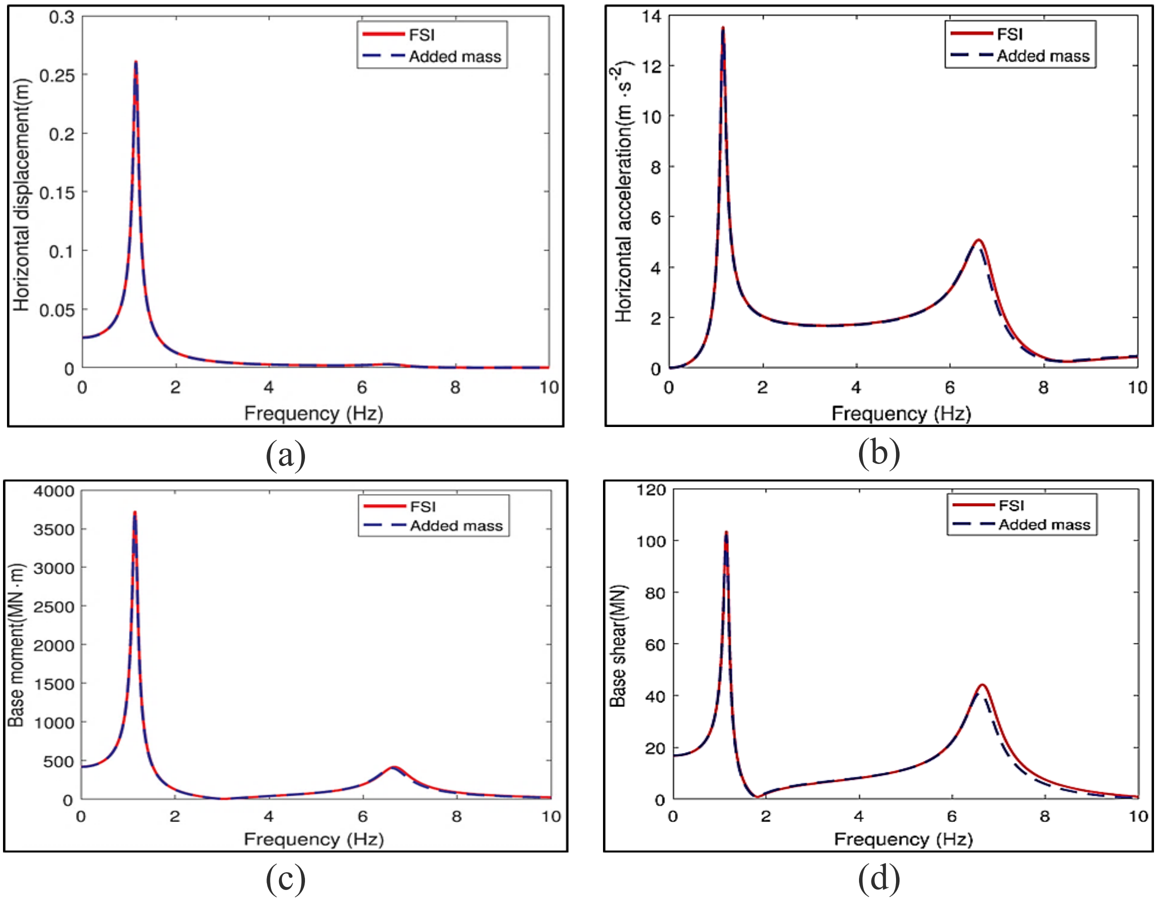

Figure 8: Frequency response of the studied bridge pier as a function of the harmonic excitation frequency underground motion: (a) displacement at pier top; (b) acceleration at pier top; (c) base shear at the pier bottom; (d) base moment at pier bottom

3. Linear and Nonlinear Response Analysis

The proposed hybrid model investigated the effect of different current and earthquake wave effect variables on the structures. An analysis matrix was prepared to perform a parametric analysis and find the effect force's sensitivity to the variable factors. The parameters considered are water depth, current velocities, wave characteristics, and earthquake amplitudes. In particular, the study includes three different water depths, two different current speeds, three different wave characteristics, and two different amplitudes, as shown in Table 1.

Table 1: Considered forces for linear and nonlinear behavior

Water height (m)		Water current (m/sec)		Water waves (depth m, length m, period sec)		Earthquake amplitudes (g)	
H1	12	C1	1	W1	0.4, 1, 6	A1	0.1
						A2	0.2
H2	13.5	C2	2	W2	0.4, 2, 3	A3	0.3
						A4	0.4
H3	15			W3	0.6, 1, 3	A5	0.5
						A6	0.6

As earthquake amplitudes grow from Figures 9 (a to f), linear or nonlinear responses increasingly increase (PGA). The nonlinear responses of the pier are in good agreement with the linear responses when PGA is equal to 0.1 g. This suggests that even in such a situation, the pier was flexible. However, the pier entered a nonlinear condition with a rise in PGA, and its reactions were less than in linear circumstances. In particular, the nonlinear responses of base shear and base moment were much less than the linear values when PGA went up to 0.6 g.

The maximum difference between the linear and nonlinear base shear response under 0.1, 0.2, 0.3, 0.4, 0.5, and 0.6g ground motions are approximately 0%, 0.8%, 1.5%, 3.2%, 5.6 and 12%, respectively, whereas for base moment are 0%, 1.2%, 3.5%, 7.8%, 11.4 and 15%, respectively. Thus, structural non-linearity cannot be neglected in dynamic analyses of piers subjected to strong ground motion.

The results also showed that the dynamic response of the bridge pier for linear and nonlinear base shear and base moment relative is changed in a very clear way. Furthermore, it can be seen that the water height, H2, 13.5m, is distinguished by the increase in dynamic behavior compared with the other water heights taken in the present study. This is due to the large concrete mass affected by the applied water mass, where the pile cap's mass is the largest compared to the other bridge members represented by the pier and the piles. From the foregoing, it can be concluded that the pier with a pile foundation bridge submerged in great water depths leads to a greater nonlinear deformation, and the possibility of damage is higher than that of land bridges. It can be seen that the water forces represented by currents and waves have an effect that is impossible to neglect in the case of calculating the non-linear behavior of marine structures. The effect of water currents ranges from 6% to 12%, while the effect of the waves ranges from 10% to 20%. The nonlinear impacts on the dynamic behavior under combination current-wave-earthquake activities were more substantial than those under only earthquakes. Thus, in dynamic assessments of piers susceptible to current-wave motion, particularly strong water wave action, structural non-linearity cannot be ignored. This discovery merits consideration in structural design.

4. Case Study

This section investigated the spans of the selected case study as a dynamic research analysis. Figure10 presents the hybrid numerical model of the discussed multi-spans pile foundation bridge pier case study. Level-layered soil covers the bedrock, and the soil's nonlinear viscous-plastic memorial yield surface model is used to explain it. Table 2 describes model parameter values in terms of soil layers. Figure 11 display model soil layers and the additional water quality considering the impact of water on the piles with the role of waves and currents. Figure 11 describes the rigidity of the lower end of the (Mild clay), which represents the natural site's rock layer.

Table 2: Model parameters of soils

Soil layers	γ_0 ($\times 10^{-4}$)	Density (Kg/m3)	Shear wave velocity (m/s)	Friction angle (°)	Depth (m)
Mud	4.0	1800	170	16	4
Silt	4.0	1890	190	16	10
Green gray	3.7	1900	210	24	12
Brown clay	3.7	1960	260	24	14
Clay	3.8	1970	320	21	6
Mild clay	4.4	2030	380	21	8

Regarding the boundary conditions, the lower face of mild clay is impacted by earthquake action (0.3 and 0.6g as earthquake accelerations and 10Hz as earthquake frequency). Considering the nonlinear of the soil and the concrete, the linear and nonlinear, in terms of pier top displacement, acceleration, shear, and moment, for the pointed bridge pier in Figure 11, are analyzed in deep water for the impact loads of 13.5 as a water depth, 2m/sec as a current velocity, and 0.6m, 1m and 3sec as wave depth, length and period, respectively.

The hydrodynamic pressure alters the structural response characteristics of the model based on the additional water quality as a result of combined current-wave excitation and earthquake excitation. It enhances the peak displacement and acceleration of the pier top and shear and moment of the pier bottom. When analyzing the results of the study case model, it can be observed that the linear pier top amplitude waves had a greater nonlinear response which can be seen in Figure 12 (a-d). it can be seen that by increasing the acceleration from 0.3g to 0.6g, the difference between linear and nonlinear behavior increases dramatically, as presented in Figure 13(a-d). As a result, it's important to consider nonlinear dynamic responses for deepwater bridge structures in coastal environments. Neglecting the nonlinear reaction of the soil and concrete might underestimate their dynamic response, which is unsafe. To better conform to the actual circumstances, it is also vital to consider the linear and nonlinear dynamic response impact in the structural bridge design.

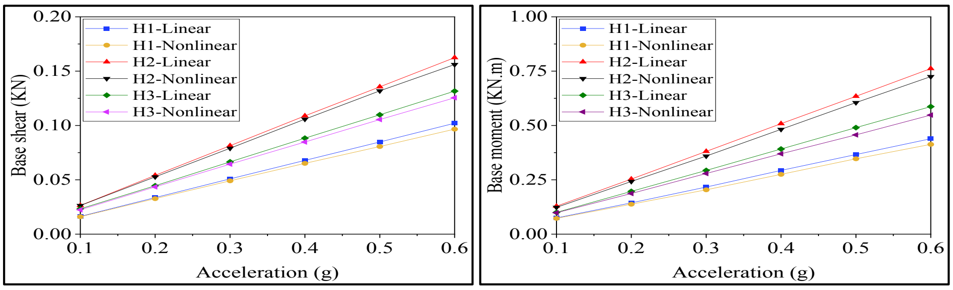

(a) C1W1

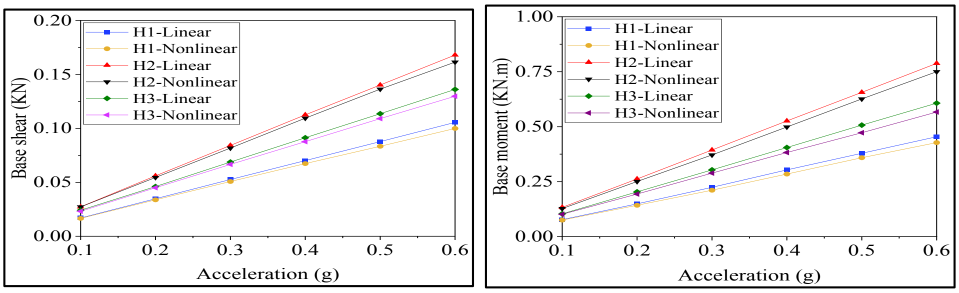

(b) C1W2.

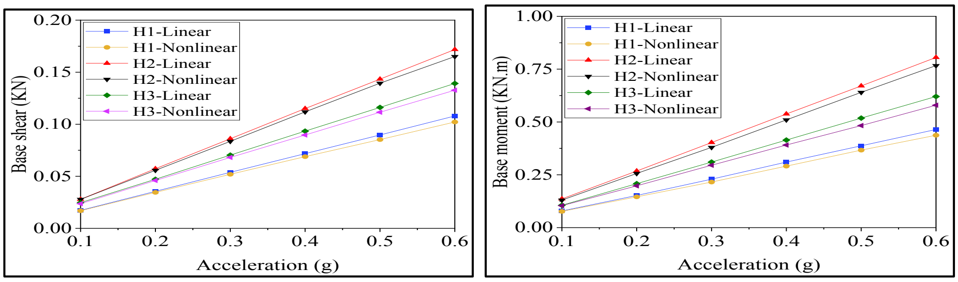

(c) C1W3.

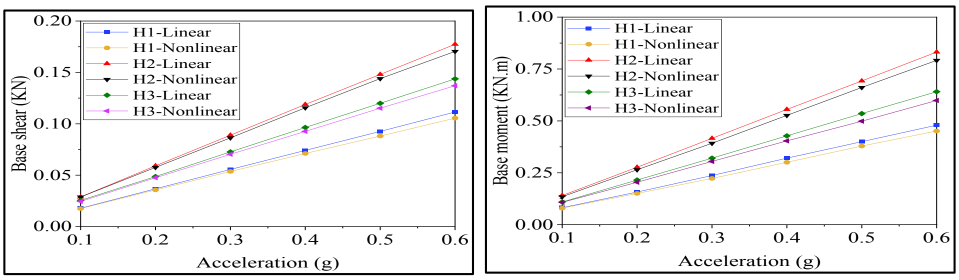

(d) C2W1.

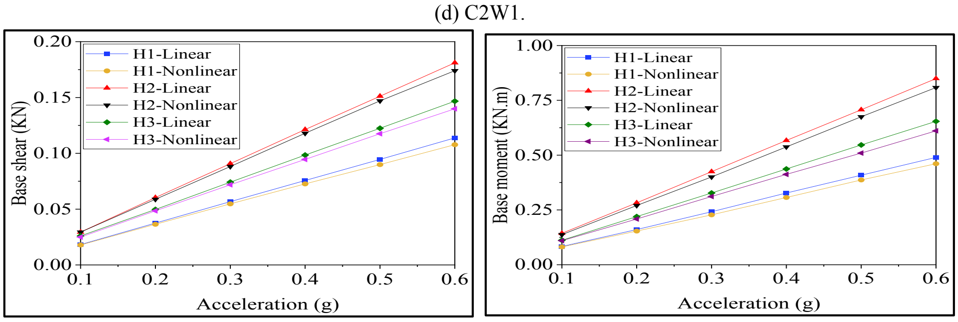

(e) C2W2.

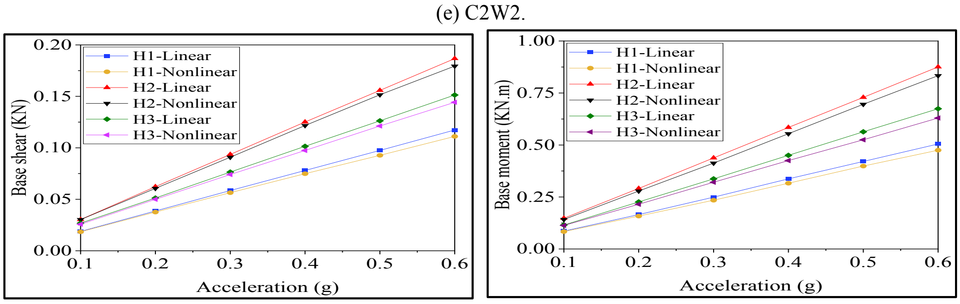

(f) C2W3.

Figure 9: Linear and nonlinear dynamic responses (shear & moment) under effect of: (a) C1W1; (b) C1W2; (c) C1W3; (d) C2W1; (e) C2W2; (f) C2W3

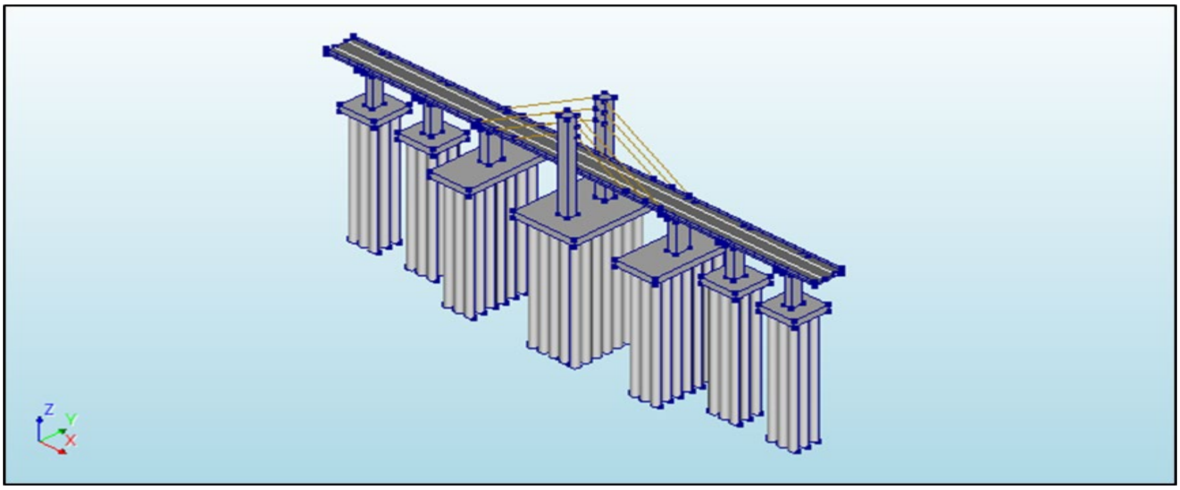

Figure 10: 3D view of the case study

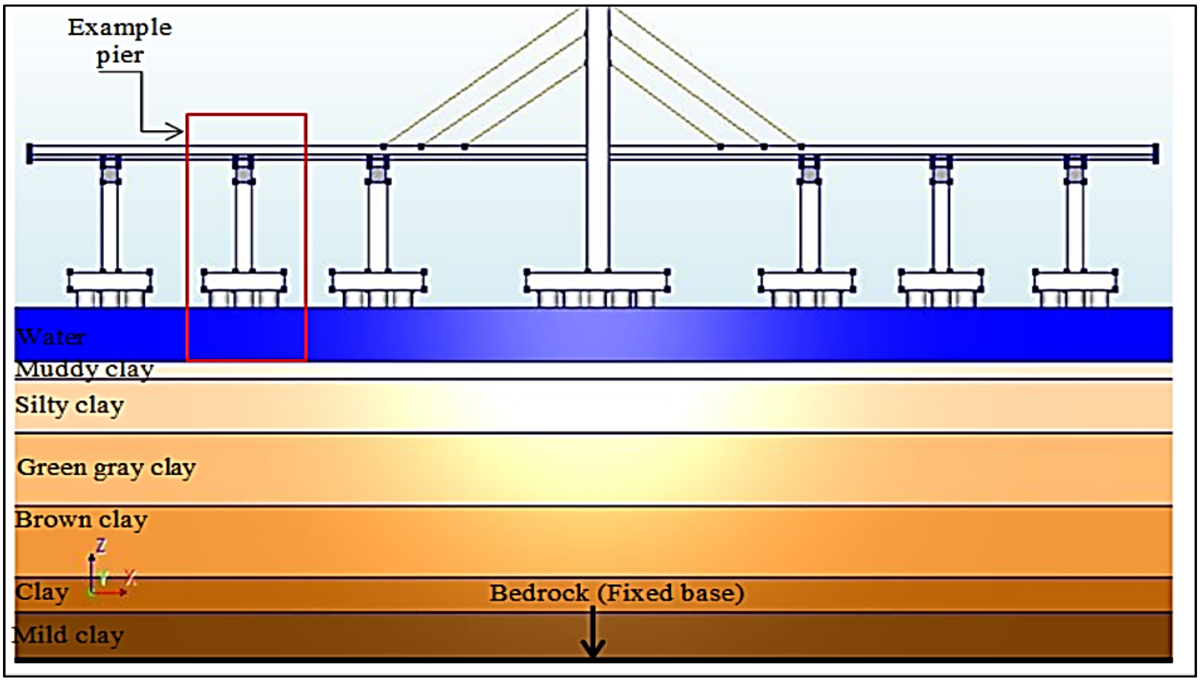

Figure 11: Model soil layers arrangements

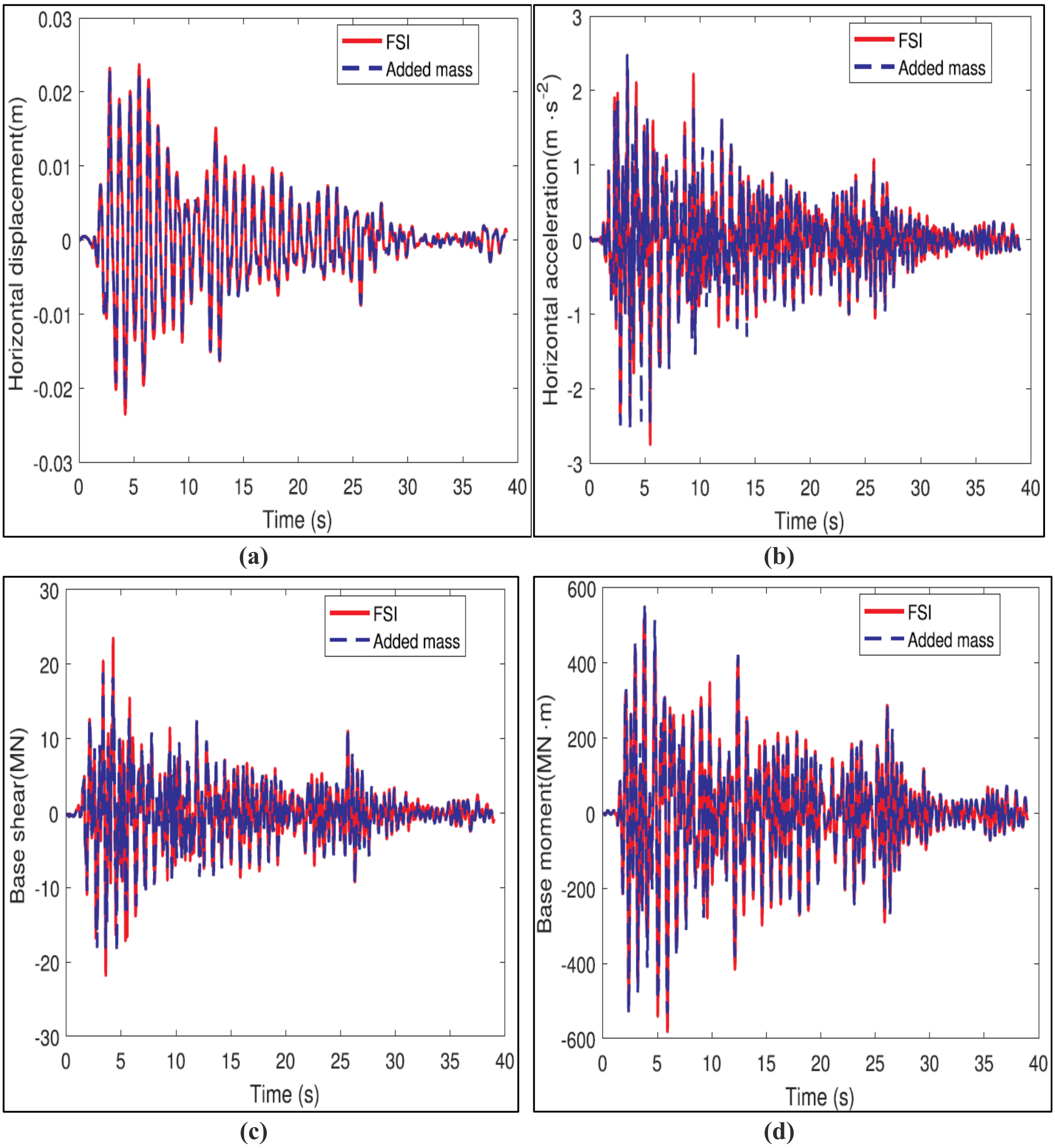

Figure 12: Time-histories of the linear and nonlinear dynamic responses of the pier top under 0.3g earthquake excitation : (a) displacement at pier top; (b) acceleration at pier top; (c) base shear at pier bottom; (d) base moment at pier bottom

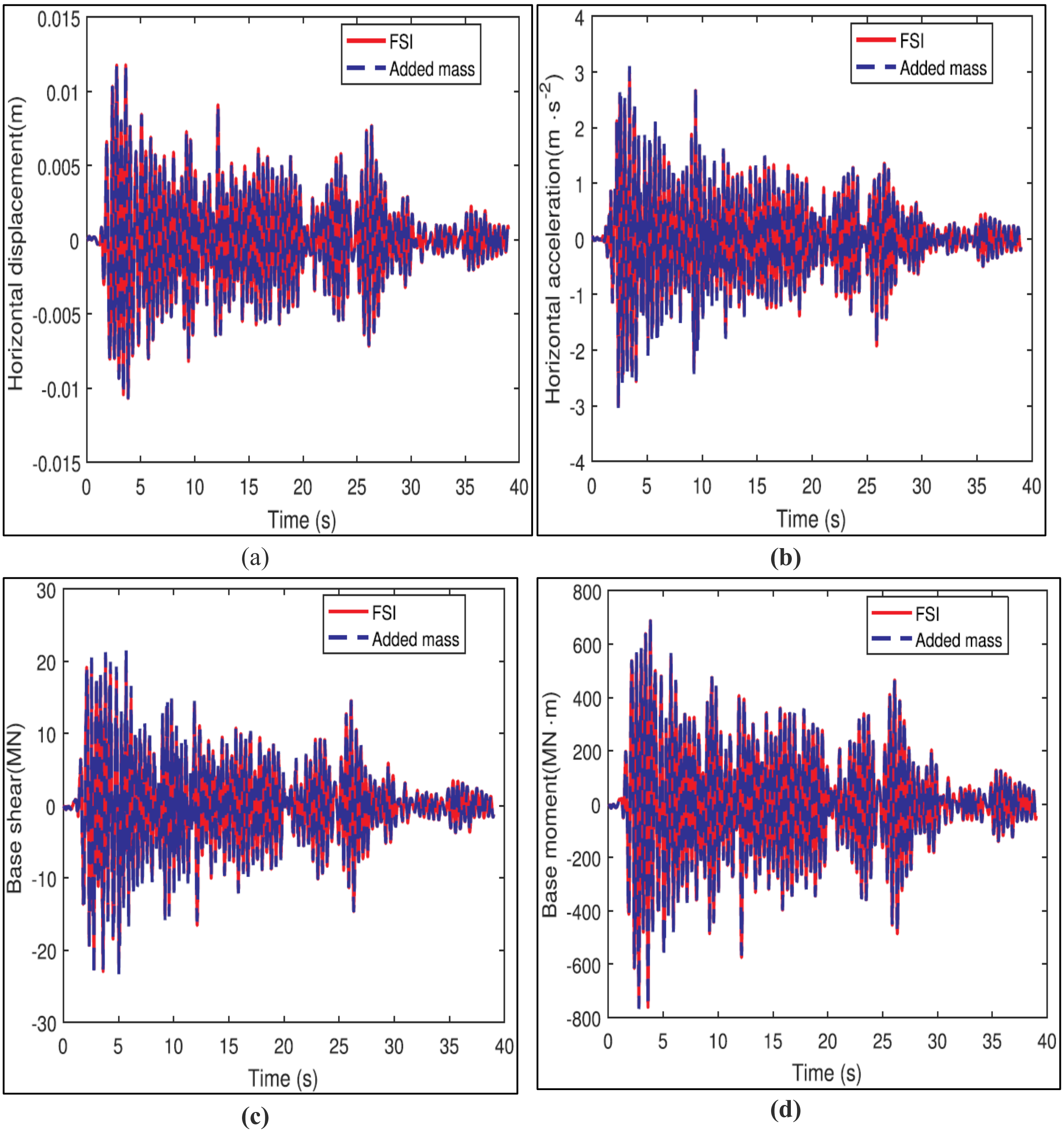

Figure 13: Time-histories of the linear and nonlinear dynamic responses of the pier top under 0.6g earthquake excitation : (a) displacement at pier top; (b) acceleration at pier top; (c) base shear at pier bottom; (d) base moment at pier bottom

5. Conclusions

This work evaluated the dynamic response of the combined impacts of current-wave and earthquake activities on a representative pile foundation bridge pier. Using coupled MATLAB and ABAQUS software, a hybrid numerical model was constructed and verified against previous experimental and developed added mass results. The general formulations of the current, wave, and earthquake were derived. The parametric study was conducted by varying water depth, current velocity, wave properties, and earthquake amplitude. Linear and nonlinear dynamic responses were presented in terms of displacement, acceleration, shear, and moment of the model-water interaction system. Based on the findings of the analysis, the following broad conclusions are drawn:

1) The efficiency of the hybrid model was demonstrated by good agreements with outcomes from earlier experimental efforts in the literature. Additionally, there was good agreement between the findings of earlier experiments and the suggested model.
2) The nonlinear responses of the pier are in good agreement with the linear responses when PGA is equal to 0.1 g. The pier entered a nonlinear condition with a rise in PGA, and its reactions were less than in linear circumstances. When PGA increased up to 0.6 g, the nonlinear behavior of base shear and the base moment was much lower than the linear values.
3) The dynamic response of the bridge pier for linear and nonlinear base shear and base moment relative is changed in a very clear, especially with an increase in the water depth compared to the other impact factors. Therefore, when the bridge is submerged in great water depths, this leads to a greater nonlinear deformation, and the possibility of damage is higher than that of land bridges.
4) These dynamic results show that the hybrid model can accurately predict the hydrodynamic pressure caused by earthquakes for pile foundation bridges. Additionally, the suggested approach eliminates the significant work required for modeling and solving complex FSI equations while yet allowing the use of additional mass in the seismic design of coastal structures.

It should be mentioned that this study still has a lot of limitations. To enhance the present model, other modeling parameters, such as the geometry of the seabed or river valley, the impact of the nearby piers, and the impact of the mountains and waves, warrant need further investigation. In addition, it is necessary to conduct probabilistic seismic evaluations of the bridge to draw broad statistical conclusions. Although there hasn't been nearly enough research on the FSI of bridges submerged in reservoirs, the hybrid FE and added-mass model confirmed in this study provide references for the hydrodynamic impacts on the seismic responses of the piled pier. They can also be helpful for the seismic design of bridges in coastal areas.

Acknowledgments

Not applicable.

Author contribution

All authors contributed equally to this work.

Funding

This research received no specific grant from any funding agency in the public, commercial, or not-for-profit sectors.

Data availability statement

The data that support the findings of this study are available on request from the corresponding author.

Conflicts of interest

The authors declare that there is no conflict of interest.

References

[1] S. S. AbdelSalam, S. Sritharan, and M. T. Suleiman, Current design and construction practices of bridge pile foundations with emphasis on implementation of LRFD, J. Bridg. Eng.,15 (2010) 749-758. https://doi.org/10.1061/(ASCE)BE.1943-5592.0000118

[2] Wei K, Yuan W, Bouaanani N. Experimental and numerical assessment of the three-dimensional modal dynamic response of bridge pile foundations submerged in water, J Bridg. Eng., 18 (2013) 1032–1041.

[3] Wei C ,Numerical simulation of combined actions of wind and wave and their actions on cylindrical component. Harbin Institute of Technology, Harbin,2012.

[4] W.Yang, Q.Li, and H.Yeh, Calculation method of hydrodynamic forces on circular piers during earthquakes, J. Bridge Eng., 22 (2017) 04017093. http://dx.doi.org/10.1061/(ASCE)BE.1943-5592.0001119

[5] W. An-jie, and Y. Wan-li, Numerical study of pile group effect on the hydrodynamic force on a pile of sea-crossing bridges during earthquakes, Ocean Eng., 199(2020) 106999. https://doi.org/10.1016/j.oceaneng.2020.106999

[6] A. Uściłowska , J.A. Kołodziej, Free vibration of immersed column carrying a tip mass, J. Sound Vib., 216 (1998) 147–157. https://doi.org/10.1006/jsvi.1998.1694

[7] Q. Yue & x. Bi, ice-induced jacket structure vibrations in bohai sea, J. Cold. Reg. Eng., 14 (2002) 81-92. https://doi.org/10.1061/(ASCE)0887-381X(2000)14:2(81)

[8] Z. Yunliang Li Zhijun and Lin Gao .Ice-structure, dynamic interaction process of DDA simulation. Glacier frozen soil, 25 (2003) 313-316.

[9] Liu. Chuanguang . Bridge construction response in the earthquake and ice loads, Earthq. Eng. Eng. Vib., 25 (2005),141-146.

[10] Huang Xin. Seismic excitation-water and pier dynamic interaction analysis, Tianjin University,2008.

[11] Gao Xuekui, Zhu Xi, and Li Hui. The seismic response analysis of the deep water bridge pier under Near-field seismic wave, Engineering seismic and reinforcement and reconstruction, 28 (2009) 83-87.

[12] Pei. Bing, Seismic dynamic response of Hardfill dam comparative analysis, Hydropower energy science, 28 (2010) 85-88.

[13] Q.Li and W.Yang, An improved method of hydrodynamic pressure calculation for circular hollow piers in deep water under earthquake, Ocean Eng., 72 (2013) 241-256. https://doi.org/10.1016/j.oceaneng.2013.07.001

[14] Jiang, H., Wang, B., Bai, X., Zeng, C. and Zhang, H. Simplified expression of hydrodynamic pressure on deepwater cylindrical bridge piers during earthquakes, J. Bridge Eng., 22 (2017a) 04017014 https://10.1061/(ASCE)BE.1943-5592.0001032

[15] P. Wang, M. Zhao and X.Du, Analytical solution and simplified formula for earthquake induced hydrodynamic pressure on elliptical hollow cylinders in water, Ocean Eng., 148(2018) 149-160. https://doi.org/10.1016/j.oceaneng.2017.11.019

[16] J.Wang, T. Zhang, M. X., A. Y. Jin, and C. H. Zhang, Seismic fragility of arch dams based on damage analysis. Soil Dyn. Earthq. Eng., 109 (2018) 58-68. https://doi.org/10.1016/j.soildyn.2018.01.018

[17] He. Xu, D. Zou, X. Kong, , Hu, Z., Su, X. A nonlinear analysis of dynamic interactions of CFRD–compressible reservoir system based on FEM–SBFEM, Soil Dyn. Earthq. Eng., 112 (2018) 24–34. https://doi.org/10.1016/j.soildyn.2018.04.057

[18] L.Yingyi, HAMS:a requency-domain preprocessor for wave-structure interactions—theory, development, and application, J. Mar. Sci. Eng., 7 (2019) 81. https://doi.org/10.3390/jmse7030081

[19] H. Gou, h. Long, y. Bao, g. Chen, q. Pu, and r. Kang, Stress distributions in girder-arch-pier connections of long-span continuous rigid frame arch railway bridges, J. Bridge Eng., 23 (2018) 7-22. https://doi.org/10.1061/(ASCE)BE.1943-5592.0001250

[20] H. Jiang, B. X. Wang, X. Bai, and C. Zeng, Nonlinear, dynamic response character of deep-water bridge piers excited by strong near-fault and far-field earthquakes, J. Huazhong Univ. Sci. Technol., 45 (2017) 81-86.

[21] Pang, Y., Kai, W., Yuan, W. and Shen, G. Effects of dynamic fluid-structure interaction on seismic response of multi-span deep water bridges using fragility function method, Adv. Struct. Eng., 18 (2015) 525-541.

[22] H.M.Westergaard,Water pressures on dams during earthquakes. ASCE Transactions., 98 (1933) 418-433. https://doi.org/10.1061/TACEAT.0004496

[23] W.Yang, and Q.Li, The expanded Morison equation considering inner and outer water hydrodynamic pressure of hollow piers, Ocean Eng., 69 (2013) 79-87. https://doi.org/10.1016/j.oceaneng.2013.05.008

[24] Ministry of Communications of China. Code for design of ground base and foundation of highway bridges and culverts. JTG D63-2007, China Communications Press, Beijing (in Chinese),2007.

[25] Gruber JJ. Reliability and effect of partially restrained wood shear walls. Wayne State University dissertations. Paper 442,2012.

[26] Abaqus Analysis User's Manual. Version 6.11, Formulation of Eulerian– Lagrangian contact Section 14.1.1. Dassault Systèmes,2011

[27] A. J. Al-Taie, and B. S. Albusoda, Earthquake hazard on Iraqi soil: Halabjah earthquake as a case study, Geod. Geodyn., 10 (2019) 196-204. https://doi.org/10.1016/j.geog.2019.03.004

[28] MCPRC, Ministry of Communications of the People's Republic of China. Code for design of highway reinforced concrete and pre-stressed concrete bridge and culverts. JTGD62-2004. Beijing: China Communications,2004.

[29] K.-J. Bathe, J. Walczak, A. Welch, and N. Mistry ,Nonlinear analysis of concrete structures, Comput. Struct., 32 (1989) 563–590. https://doi.org/10.1016/0045-7949(89)90347-7

[30] D.Khatri, and J. C. Anderson, Analysis of reinforced concrete shear wall components using the ADINA nonlinear concrete model, Comput. Struct., 56 (1995) 485–504. https://doi.org/10.1016/0045-7949(95)00039-J

[31] M. Mao, and C. A. Taylor, Non-linear seismic cracking analysis of medium-height concrete gravity dams. Comput. Struct., 64 (1997) 1197–1204. https://doi.org/10.1016/S0045-7949(97)00029-1

[32] J. B. Mander, M. J. N. Priestley, and R. Park, Theoretical stressstrain model for confined concrete, J. Struct. Eng., 114 (1988) 1804–1826. https://doi.org/10.1061/(ASCE)0733-9445(1988)114:8(1804)

[33] Yang, W.L., Li, A., Li, Q., Wen, Z.B., Zhao, W.L. (2018). Scaling law study for earthquake induced pier–water interaction experiments, Environ. Fluid Mech., 19 (2019), 55–79. https://link.springer.com/article/10.1007/s10652-018-9618-4

[34] W.Yang, Study on hydrodynamic analysis methods of deep-water bridges, [In Chinese.] thesis, (2012, Southwest Jiaotong University.

[35] J. Zhang, K. Wei, Y. Pang, M. Zhang, & S.Qin, Numerical investigation into hydrodynamic effects on the seismic response of complex hollow bridge pier submerged in reservoir: case study. J. Bridge. Eng., *24*(2019) 05018016. https://doi/abs/10.1061/(ASCE)BE.1943-5592.0001340

[36] Ministry of Transport of the People’s Republic of China (2015). JTS145-2015 Code of Hydrology for Harbour and Waterway[S]. China Communications Press, Beijing,2015.